Case studies of mirror-mode structures observed by THEMIS in the near-Earth tail during substorms

Y. S. Ge,[1] J. P. McFadden,[2] J. Raeder,[1] V. Angelopoulos,[3] D. Larson,[2] and O. D. Constantinescu[4]

Received 8 April 2010; revised 4 November 2010; accepted 10 November 2010; published 21 January 2011.

[1] An examination of the magnetic field and plasma observed by the inner THEMIS-D spacecraft (P3) close to the equatorial plane at ~11R_E at local midnight reveals the occurrence of mirror-mode structures. These structures have the same characteristic waveform seen in other regions. The examination of the mirror-mode instability shows that inside these structures the threshold of mirror instability is marginally reached, while the surrounding plasma is mirror stable. The observed mirror structures occur in the dipolarized magnetic field following a substorm-related dipolarization. It is found that after the dipolarization front, the local ions become more anisotropic and initial magnetic holes form inside this anisotropic plasma before the fully-fledged mirror structures are observed. The ions become less anisotropic afterward, but the strong field depression in the magnetic holes enhances the effective plasma beta so that the mirror instability threshold is marginally reached. Thus, the dipolarization process provides the large-amplitude magnetic field fluctuations and the anisotropic plasma environment for mirror structures to grow. The isolated large-amplitude mirror-mode structures survive in the mirror-stable plasma even through the plasma becomes less anisotropic. It is also found that the width of magnetotail mirror-structures is smaller than one gyroradius of a plasma sheet proton, which is different from the width of mirror structures in other regions. These mirror structures appear to have a strong correlation with electron anisotropy changes. These observations suggest that electron kinetics may also play a role during the growth and saturation of mirror instability in the near-Earth tail.

Citation: Ge, Y. S., J. P. McFadden, J. Raeder, V. Angelopoulos, D. Larson, and O. D. Constantinescu (2011), Case studies of mirror-mode structures observed by THEMIS in the near-Earth tail during substorms, *J. Geophys. Res.*, *116*, A01209, doi:10.1029/2010JA015546.

1. Introduction

[2] Magnetic mirror instability [*Hasegawa*, 1969; *Kivelson and Southwood*, 1996; *Southwood and Kivelson*, 1993] occurs in anisotropic plasmas with high β value. It purely grows in the frame of reference of the plasma and results in a nonpropagating mirror-mode wave [*Southwood and Kivelson*, 1993; *Tajiri*, 1967]. Mirror-mode waves are often found in the terrestrial magnetosheath [*Crooker and Siscoe*, 1977; *Lucek et al.*, 2001; *Tsurutani et al.*, 1982; *Constantinescu et al.*, 2003]. Mirror instability has also been observed near Jupiter [*Russell et al.*, 1999], in the Venus magnetosphere [*Volwerk et al.*, 2008], near comets [*Russell et al.*, 1987; *Glassmeier et al.*, 1993; *Tsurutani et al.*, 1999] and in the solar wind [*Winterhalter et al.*, 1994; *Zhang et al.*, 2008, 2009; *Russell et al.*, 2009]. However, inside the Earth's magnetosphere, reports of mirror-mode waves are rare and most observations of mirror-mode waves are drift mirror-mode waves. They are found, for example, in the ring current region [*Woch et al.*, 1988], on the magnetospheric flanks [*Zhu and Kivelson*, 1991, 1994; *Constantinescu et al.*, 2009], and in the dawnside plasma sheet [*Vaivads et al.*, 2001]. Recently a series of mirror-mode waves were observed by *Rae et al.* [2007] with observations from the Equator-S spacecraft. These mirror waves were found to be coupled with standing shear Alfven waves and excite the compressional Pc5 waves in the dawnside flank on the equatorial plane [*Rae et al.*, 2007]. This study shows an excellent example of the mirror instability exciting ULF waves and demonstrates that the mirror instability may play an important role in transferring energy from hot plasma into ULF waves inside the Earth's magnetosphere.

[3] With no coupling to the drift mode or the drift Alfven ballooning mode, the mirror mode is a zero frequency

[1]Space Science Center, University of New Hampshire, Durham, New Hampshire, USA.
[2]Space Science Laboratory, University of California, Berkeley, California, USA.
[3]Institute of Geophysics and Planetary Physics, University of California, Los Angeles, California, USA.
[4]Institut für Geophysik und Meteorologie, Technische Universität Braunschweig, Braunschweig, Germany.

0148-0227/11/2010JA015546

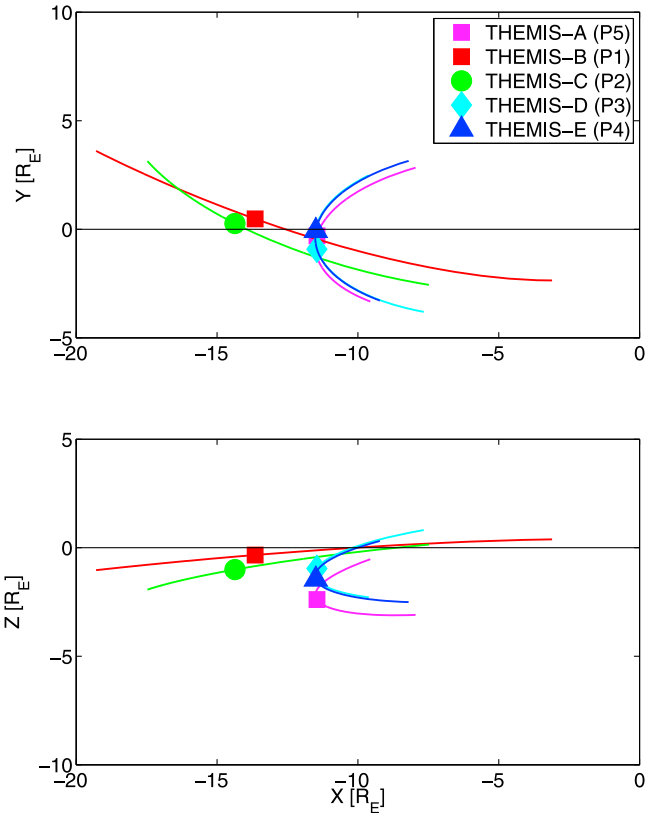

Figure 1. Projections of THEMIS spacecraft orbits on the noon-midnight meridian and the equtorial planes in GSE coordinates on 15 March 2009. The symbols indicate the positions of five spacecraft at 0800 UT.

standing mode. The magnetic field signature in this standing mode is manifested as isolated magnetic peaks (magnetic field enhancements) or holes (magnetic field depressions) superposed upon a relatively flat background. The magnetic holes have been well studied in the solar wind [*Stevens and Kasper*, 2007, and references therein] and the magnetosheaths [*Joy et al.*, 2006; *Soucek et al.*, 2008, and references therein]. In the planetary magnetosheaths, the pressure anisotropy is generated as the plasma flow moves through the bow shock where the ion temperature increases with a larger proportion of heating preferentially going to the perpendicular component [*Pokhotelov et al.*, 2001; *Liu et al.*, 2005]. Close to the bow shock, mirror modes are generated and appear as quasi-sinusoidal waves in the early stages of development. They approach nonlinear saturation further downstream of the bow shock [*Soucek et al.*, 2008]. In this region, the mirror modes change into nonperiodic structures with large-amplitude fluctuations of the magnetic field, i.e., magnetic peaks and holes. Usually magnetic peak-type and hole-type mirror structures manifest themselves as sporadically distributed magnetic field peaks and holes superposed on a gradually varying background field, respectively. They can be identified on the time series of the magnetic field by sudden and strong enhancements and depressions in the magnetic field strength. Recently *Soucek et al.* [2008] and *Genot et al.* [2009] statistically investigated the relation of forms of mirror-mode structures with the plasma parameters such as the plasma beta (β) and anisotropy using Cluster observations. They found that magnetic peaks are typically observed in a mirror unstable plasma, while magnetic holes are observed deep within the stable region where magnetic peaks rapidly decay. From these observations, an evolution model of mirror modes in the magnetosheath is proposed, where large magnetic peaks grow out from a moderately unstable plasma (typically behind the bow shock). As the plasma β further decreases closer to the magnetopause, the plasma becomes mirror stable. In this region magnetic peaks are heavily damped while magnetic holes survive. *Hellinger et al.* [2003] and *Travnicek et al.* [2007] show consistent results by studying the effect of plasma compression and expansion on the mirror and ion cyclotron instabilities using hybrid simulations. More recent studies using Time History of Events and Macroscale Interactions during Substorms (THEMIS) observations performed by *Balikhin et al.* [2009] on the dayside magnetosheath indicates that some mirror structures appear to be surrounded by mirror stable plasma.

[4] The near-Earth tail region is interesting since it includes the transition of the magnetic field from a tail-like to a dipolar field configuration. Observations from Active Magnetospheric Particle Tracer Explorers/Charge Composition Explorer (AMPTE/CCE) found that the plasma pressure could be strongly anisotropic in this region ($X > -15\ R_E$) and the anisotropy increased toward the Earth [*Lui and Hamilton*, 1992]. Within $L \sim 9$, the anisotropy is always below the firehose instability threshold during quiet times and near the mirror instability threshold in the midnight sector at large L shells [*Lui and Hamilton*, 1992]. However, from AMPTE/CCE charge-energy-mass (CHEM) measurements the plasma anisotropy is very small near the midnight sector for $L > 8$, while the plasma is generally anisotropic in the flanks [*De Michelis et al.*, 1999]. *De Michelis et al.* [1999] also pointed out that the plasma anisotropy is generally greater during nightside active times (AE > 100 nT) than quiet times. Non-oscillary mirror-mode structures have also been observed inside the Earth's magnetosphere using Equator-S and Cluster observations and were described as plasma blobs [*Haerendel et al.*, 1999, 2004]. *Haerendel et al.* [1999] suggested that the plasma blobs had their source in the morningside boundary layer, although they also proposed that these structures might also be related to substorm activity [*Haerendel*, 2000]. However, these observations from Equator-S spacecraft were made in the morningside of magnetosphere, and the plasma anisotropy in this region is usually different from that in the sector close to midnight where most manifestations of substorms exist [*De Michelis et al.*, 1999]. Substorms produce strong dipolarizations of the magnetic field near the midnight sector, which can modify the properties of local plasma in the near-Earth tail region. Thus, our investigation of mirror structures during substorms addresses the generation of mirror instability inside magnetosphere and within the general isotropic plasma environment.

[5] In this study, we use THEMIS observations during two orbits in its second tail season to investigate the plasma and magnetic field conditions during substorms in the midnight sector. Structures associated with mirror-mode instability are found after the near-Earth dipolarization. The mirror-mode instability criteria was marginally reached in

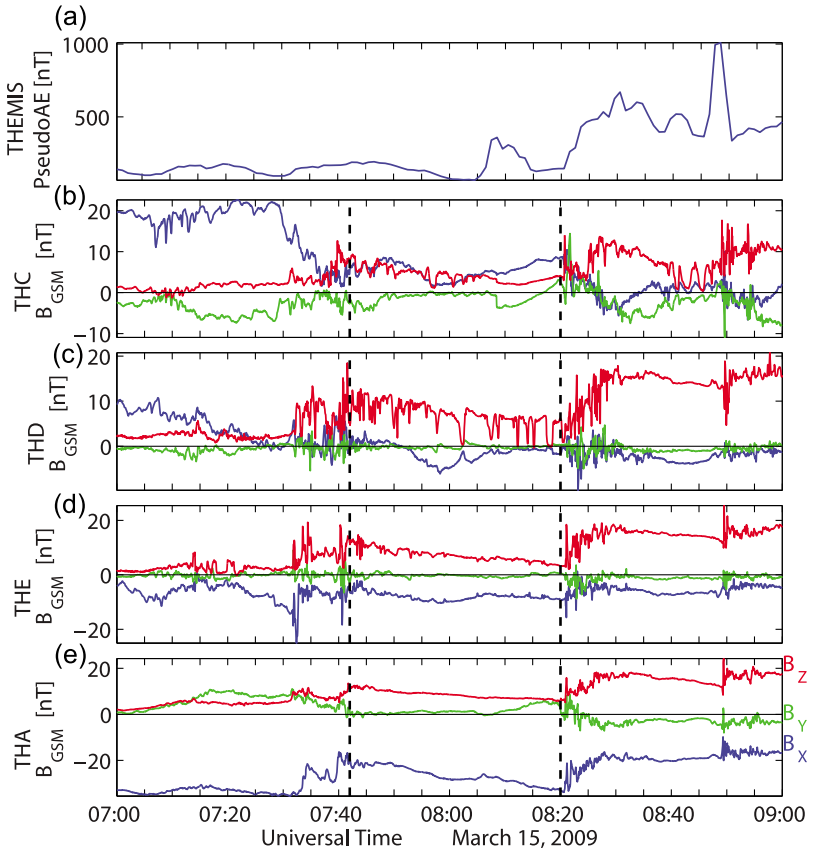

Figure 2. (a) THEMIS pseudo-AE index shows a substorm onset at 0804 UT and a pseudo-onset at 0730 UT on 15 March 2009. Three components of the magnetic field in GSM coordinates for THEMIS spacecraft (b) C, (c) D, (d) E, and (e) A (from midtail to near-Earth tail). Two dipolarizations are shown on each of the four spacecraft at 0732 and 0820 UT. The two dashed lines show the intervals of the mirror structures.

these magnetic holes while the background plasma remained mirror stable, which provided a favorable condition for mirror-mode waves to develop. We find that the dipolarization prior to these structures not only produces large-amplitude fluctuations in the magnetic field but also causes the local plasma to become anisotropic. We also find that the small-amplitude magnetic holes formed prior to the isolated large-amplitude mirror structures and immediately after the dipolarization. Afterwards, the plasma anisotropy decreases when the mirror structures are fully developed. The spatial scale of these structures is investigated, and the widths of mirror structures are found to be smaller than the gyroradius of a plasma sheet proton but are tens of electron gyroradii. We also found a strong correlation between these magnetic holes and the changes of electron pitch angle distributions. Despite the parallel-anisotropic electrons in the surrounding plasma, the electrons inside of the magnetic holes are isotropic.

2. Magnetic Field Observations

[6] At the end of December 2007, the THEMIS mission [*Angelopoulos*, 2008] entered its first tail season dedicated to studying the time history of substorm processes with the radial alignment of spacecraft from ~30 R_E to ~9 R_E in the magnetotail. The second tail season came in the late 2008 with modified spacecraft orbits, which enabled the outer THEMIS spacecraft (THEMIS-B (THB) and THEMIS-C (THC, i.e., P1 and P2) to cross the tail closer to the central plasma sheet than those in the first tail season. On 15 March 2009, the five THEMIS spacecraft entered one of their major conjunction configurations, shown in Figure 1. Two midtail spacecraft, THB (P1) and THC (P2), are close to each other and the innermost spacecraft approach their apogees. All spacecraft are located in the midnight sector and close to the equatorial plane. Particularly, THEMIS-D (THD, P3) is located at −11.45, −0.92, −0.96 R_E in Geocentric Solar Ecliptic (GSE) coordinates at 0800 UT.

[7] At around 0800 UT, a strong substorm occurs with the maximum AE index over 1000 nT as shown in Figure 2a. The AE index shown here is constructed using the THEMIS Ground-Based Observatories (GBO), the Education and Public Outreach (EPO) network located in Canada and Alaska [*Mende et al.*, 2008; *Russell et al.*, 2008; *Peticolas et al.*, 2008], the upgraded and expanded Canadian Array for Realtime Investigations of Magnetic Activity (CARISMA) [*Mann et al.*, 2008], Geophysical Institute Magnetometer Array (GIMA), and the Canadian CANMOS magnetometer array. The substorm also manifests itself in dipolarizations of the near-Earth tail magnetic field. Figures 2b–2e show

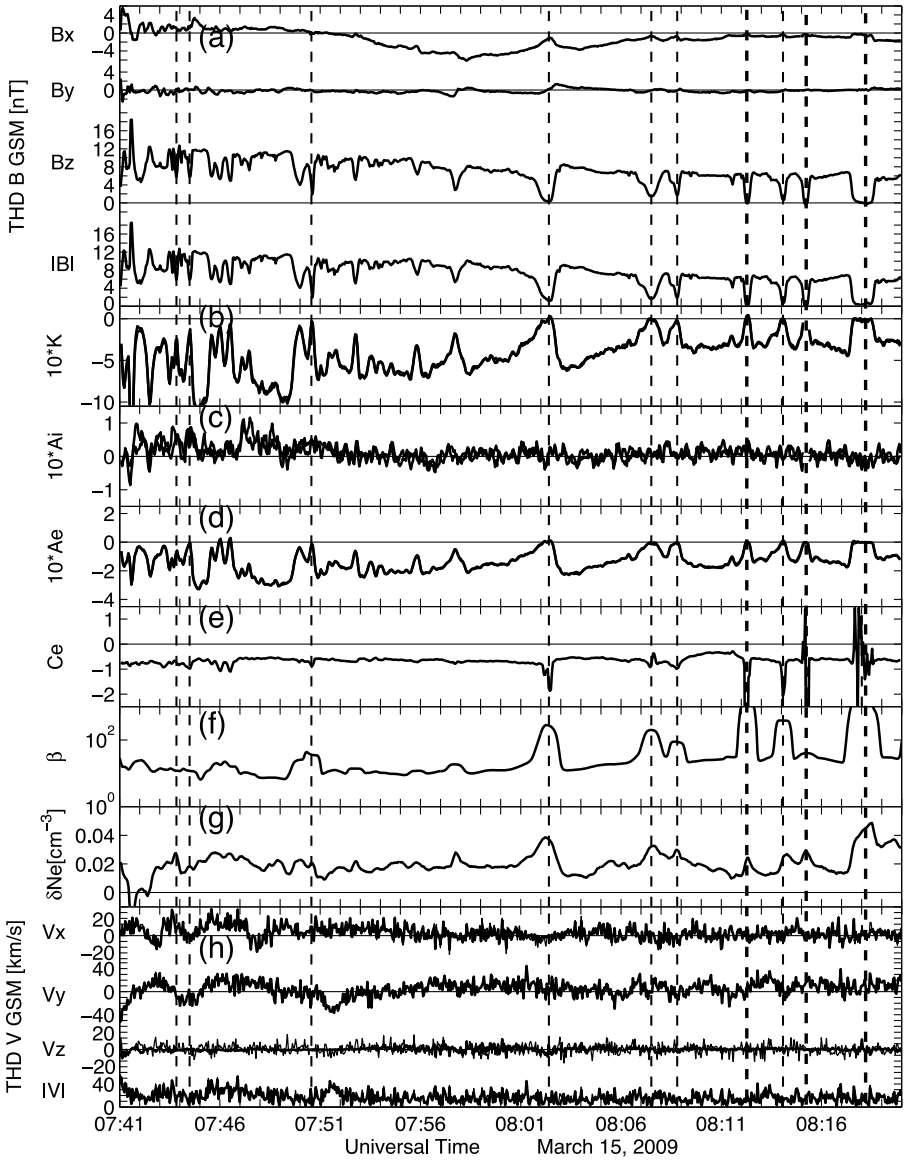

Figure 3. (a) THEMIS-D (P3) observations of the magnetic field in GSM coordinates, (b) *Ki* values (two traces corresponding to the two components of the perpendicular temperature), (c) the anisotropy of ion, (d) the electron anisotropy, (e) the fire hose instability threshold for electrons, (f) the plasma beta, (g) the variations of electron density, and (h) plasma flows are shown during the interval of mirror structures on 15 March 2009. The six thin dashed lines mark mirror-mode structures and the three thick dashed lines mark the three structures selected to calculate the width of mirror structures.

the magnetic field measurements in Geocentric Solar Magnetospheric (GSM) coordinates from all THEMIS spacecraft. Figures 2b–2e are arranged by radial distances, that is, from the midtail spacecraft THC (P2; Figure 2b) to the innermost THEMIS-A (THA, P5; Figure 2e). Multiple dipolarizations are found on all probes. The dipolarization at 0820 UT corresponds to an AE enhancement in this substorm, while according the THEMIS All-Sky-Imager observations (not shown here) the dipolarization at 0732 UT corresponds to a pseudo-onset with a small enhancement of AE index. The first dipolarization at ~0732 UT makes the near-Earth tail field more dipole (i.e., in the GSM *z* direction) where it remains post onset. The *Bz* component of magnetic field gradually declines before the second dipolarization at 0820 UT, showing another slow stretching process of tail. Large-amplitude fluctuations of the magnetic field accompany both strong dipolarizations. On top of the slowly declining background, multiple magnetic field holes are seen from ~0742 UT to the second dipolarization at 0820 UT.

[8] Figure 3 shows the detailed observations of magnetic field and plasma parameters on THD through these magnetic holes from 0742 to 0820 UT. It is found that all magnetic field components approach zero inside these magnetic holes. The background plasma bulk flow is small and mainly in the GSM *y* direction. The durations of these

magnetic holes are found to vary from less than 1 minute to several minutes. The observed time scale of these structures is determined by the spatial scale of these structures, the background plasma convection velocity, and the path of the spacecraft through them. These magnetic holes also have various amplitudes or different local minima of the magnetic field strength and are distributed sporadically in the time series. These signatures of magnetic holes are similar to the mirror-mode structures discovered in other regimes, such as in the solar wind and the cometary sheath. The sporadic distribution of magnetic holes suggests the standing mode nature of these structures. In other words, these magnetic holes are not propagating in the frame of the reference of the plasma and the temporal variations are produced by the convection of the background plasma flow and the motion of the spacecraft.

3. Mirror-Mode Instability Criteria

[9] The mirror instability condition in the cold electron bi-Maxwellian fluid approximation has been given by [*Hasegawa*, 1969] as

$$1 + \sum_i \beta_{\perp,s}\left[1 - \frac{T_{\perp,s}}{T_{\parallel,s}}\right] < 0, \quad (1)$$

where $\beta_{\perp,s} = \frac{nk_BT_{\perp,s}}{B^2/2\mu_0}$, $T_{\perp,s}$ and $T_{\parallel,s}$ are the perpendicular and parallel temperatures, respectively, and s denotes ion and electron. Although the physics of mirror instability has to be described through kinetic treatments [*Southwood and Kivelson*, 1993], the expression in (1) still presents a correct threshold in the kinetic cold electron limit. In the central plasma sheet, the electron temperature is usually about 1/7 to 1/5 of the proton temperature. *Pantellini and Schwartz* [1995] suggested that the mirror instability threshold is increased when the electron temperature T_e is of the same order of the proton temperature parallel to the background magnetic field $T_{\parallel,p}$. However, *Pokhotelov et al.* [2000] found that for the isotropic electron distribution, the modification of mirror instability threshold due to the finite electron temperature is insignificant. We use a parameter $K = T_\perp/T_\parallel - 1 - 1/\beta_\perp$, which is derived by simply rewriting the Hasegawa equation (i.e., equation (1)) to indicate the distance to the mirror instability threshold in this study; K is positive when the mirror instability threshold is reached. *Balikhin et al.* [2009; Figure 3] have shown the correlation of positive K with mirror structures in the dayside magnetosheath.

[10] In Figure 3, we used magnetic field measurements [*Auster et al.*, 2008] and electrostatic analyzer (ESA) [*McFadden et al.*, 2008] plasma data to calculate the value of K during the interval of magnetic holes. In Figure 3b (Figure 3a shows the magnetic field components and the field strength), the value of K is shown in two traces which are calculated from two components of the perpendicular temperatures of electrons and ions measured by ESA in the perpendicular plane to the ambient magnetic field orientation. It is clear from Figure 3 that during the magnetic holes the value of K is positive or close to zero, showing the plasma in these structures marginally reaches the threshold of mirror instability. However outside of these mirror structures, the plasma appears to be mirror stable (negative K). This suggests that these mirror structures are embedded in regions of mirror stable plasma, which is similar to the mirror structures observed in the dayside magnetosheath by THEMIS spacecraft [*Balikhin et al.*, 2009].

[11] Figure 3 also shows that the magnetic field depression is substantial in these structures. The magnitude of background magnetic field slowly varies from 11 nT to 7 nT. This gradual declining of background magnetic field strength is mainly caused by the decrease of the *Bz* component which is the major component of the background magnetic field. The gradual decrease of the *Bz* component corresponds to the tail stretching before the following dipolarization. This tail stretching can be more clearly seen from the nearby spacecraft THA in the last panel of Figure 2e where the *Bz* component of the magnetic field continuously decreases during two dipolarizations while the magnitude of the *Bx* component increases. Superimposed on the gradually varying background field, the magnetic field decreases to a very low magnitude within the mirror structures. The lowest magnitude of magnetic field in these magnetic holes is 0.24 nT, as low as 3% of the background magnetic field using the median background field strength of 8 nT. Such strong depression in these magnetic holes significantly enhances the effective plasma beta value, which is much higher than the surrounding plasma. In Figure 3f, we show the value of β, where $\beta = \frac{nk_BT_e+nk_BT_i}{B^2/2\mu_0}$, which is much higher inside the magnetic holes than that of the surrounding plasma. The mirror instability threshold is marginally satisfied within these structures mainly due to the enhancement of the effective plasma beta and very small plasma anisotropy. Figure 3g shows the variations of the density of electrons calculated from both ESA and Solid State Telescopes (SST) measurements. Here, by assuming plasma neutrality, we use the variations of electron density to show the variations of plasma density because the measurements of ion density have much larger uncertainties than those of electrons. The changes of plasma density are anticorrelated with the variations of the magnetic field through these magnetic holes, which is consistent with the mirror structures found in the other regimes.

[12] In Figures 3c and 3d, we show the anisotropy ($A_s = T_{\perp,s}/T_{\parallel,s} - 1$) of ions and electrons calculated from ESA measurements The temperature calculation does not include SST measurements because SST does not have adequate angular resolution and it even has some blind spots in the axial direction (close to the GSE z direction). However, we include SST measurements for the density calculation (Figure 3g) since the density calculation is not significantly affected by the angular distribution of particles. In Figure 3e, we show the firehose parameter, C_e, which is defined by $C_e = (\beta_{\parallel,e} - \beta_{\perp,e})/2 - 1$. The plasma is unstable to the firehose instability when C_e is positive. From Figure 3c it can be seen that inside the mirror structures, the ion anisotropy is small. We can find that before the large-amplitude mirror structures and after the dipolarization (0742 UT), the ion anisotropy is substantial and significantly larger than the anisotropy observed following. In the anisotropic plasma between 0742 and 0750 UT, continuous magnetic holes also appear with relatively lower amplitudes, i.e., the local minia of the magnetic

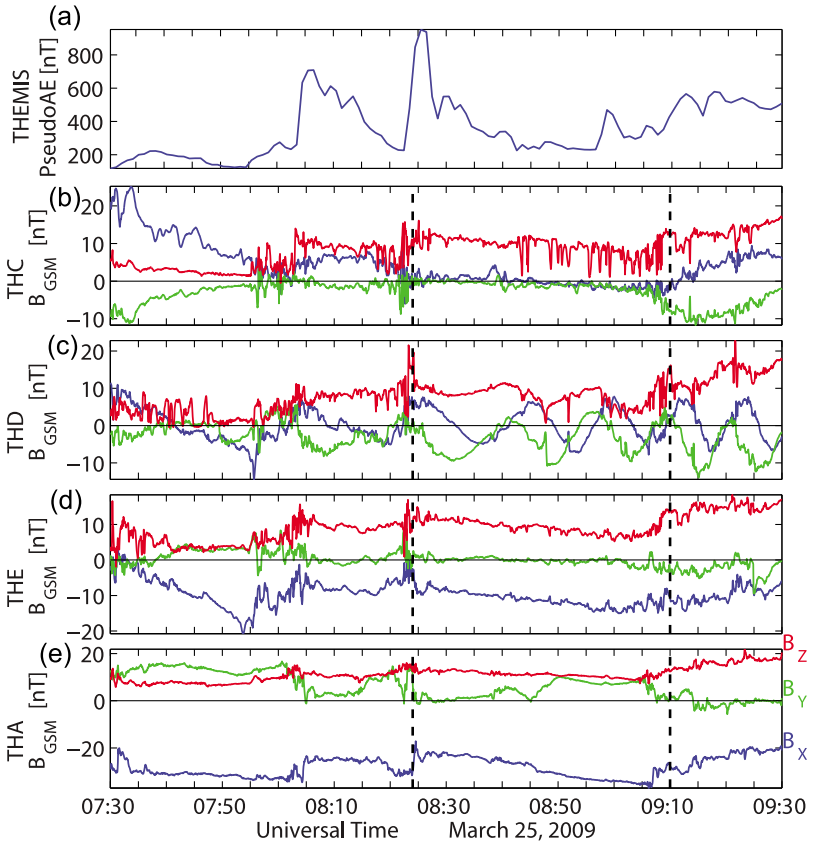

Figure 4. Overview of observations on the 25 March 2009 event. (a) THEMIS pseudo-AE index shows a substorm onset at 0804 UT and a second onset at 0824 UT. Three components of the magnetic field in GSM coordinates for THEMIS spacecraft (b) C, (c) D, (d) E, and (e) A (from midtail to the near-Earth tail). Multiple dipolarizations are shown for all four spacecraft. The two dashed lines show the intervals of the mirror structures.

field strength inside these magnetic holes is larger than those inside the following mirror structures. Note that the magnetic field strength inside these magnetic holes is still substantially low (generally lower than 50% of the background field strength), suggesting that these magnetic holes, if they are the manifestations of growing mirror-mode waves, are already in the non-linear phase. The K value during this interval (between 07:42 and 07:50 UT) remains negative. These magnetic holes also appear to be different from the following large-amplitude structures by their relatively narrower scales. However, these smaller scales in the time series are found to be temporal and probably due to the relatively higher speed of the background plasma flows. In fact, the spatial scales of these structures are found to be close to those of the large-amplitude structures, 300–600 km, using the velocity-integration method (see detailed discussion in section 4). The anticorrelation between the variations of magnetic field and plasma density can barely be seen. It is also noted that the electron anisotropy of the background plasma is in fact opposite to that of ions, with greater temperature in the direction parallel to the magnetic field. This distribution of electrons changes inside of the mirror structures and becomes isotropic. The correlation of the mirror structures and isotropic electrons is clear inside all large-amplitude structures.

[13] During another major conjunction of THEMIS spacecraft on 25 March 2009, a similar event is observed by THC (P2) further downtail. The overview plot of THEMIS spacecraft magnetic field observations and the pseudo-AE index are shown in Figure 4. There are two consecutive intensifications in AE occurring before 0830 UT and the corresponding dipolarizations are observed by THEMIS spacecraft. During the recovery phase of this substorm, multiple magnetic holes are seen on THC in the dipolarized field where the Bz component becomes the main component of magnetic field. The depression of magnetic field during these structures is also very strong, from the background field of over 10 nT to the local minima less than 1 nT. We also show the value of K, ion and electron anisotropy, the firehose instability threshold, beta and variations of electron density after the dipolarization front in Figure 5. Similar to those in Figure 3, the background plasma is moving slowly during this interval and these magnetic holes show a good correlation with the enhancements of plasma density and the marginally positive K value, suggesting that the mirror instability threshold is marginally reached in these structures. The difference between this event and the previous

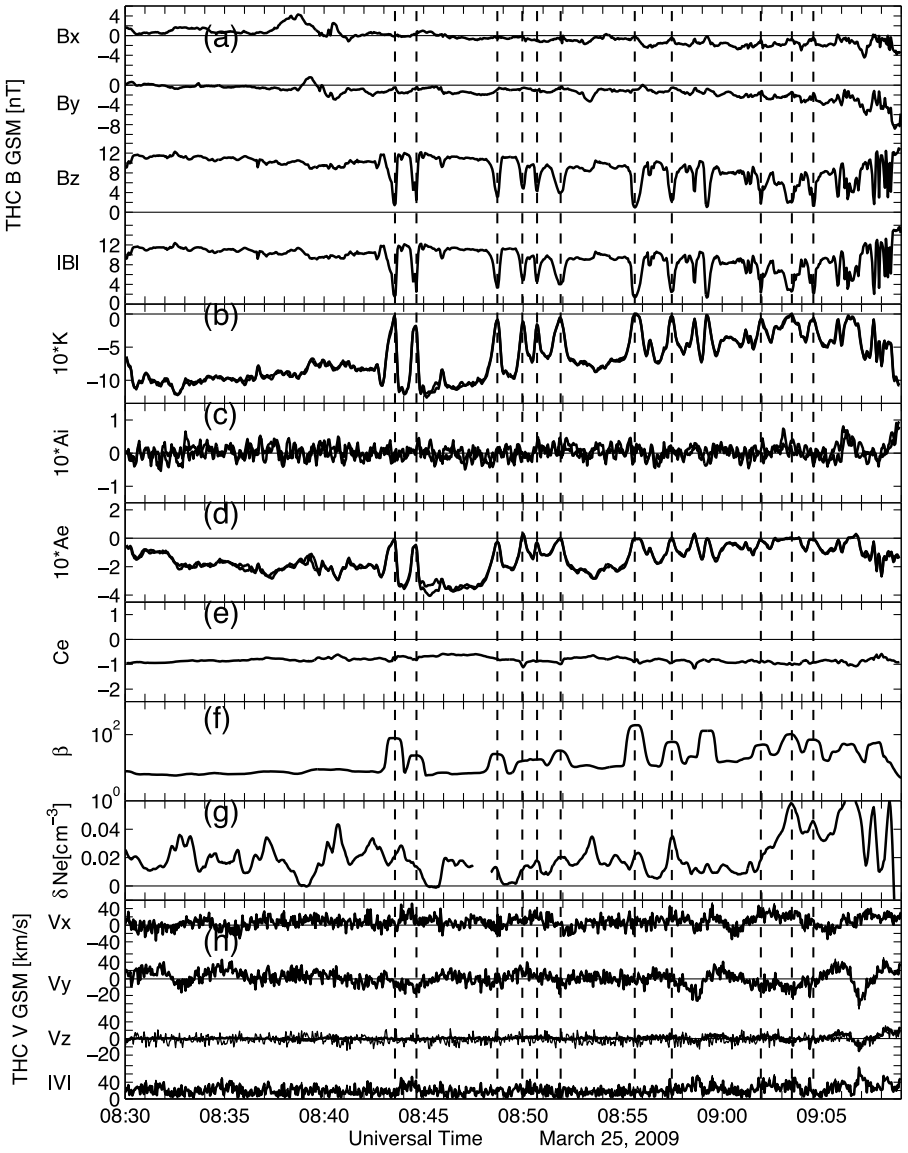

Figure 5. (a) THEMIS-C (P2) observations of the magnetic field in GSM coordinates, (b) *Ki* values (two traces corresponding to the two components of the perpendicular temperature), (c) the anisotropy of ion, (d) the electron anisotropy, (e) the firehose instability threshold for electrons, (f) the plasma beta, (g) the variations of electron density, and (h) plasma flows are shown during the interval of mirror structures on 25 March 2009. The dashed lines mark the mirror-mode structures.

one (see Figure 3) is that no clear magnetic holes are observed right after the dipolarization front. However, it still can be seen that the ions are anisotropic after the dipolarization and becomes less anisotropic when the mirror structures are observed. Another similarity is that the K value stays negative right after the dipolarization, though the ions are more anisotropic than during the mirror-structure interval. The clear correlation of magnetic holes with the isotropic electrons also appears in this event.

4. Spatial Scale of Mirror Structures and Electron Distribution

[14] In this study, THEMIS spacecraft are separated at least 1 R_E and no mirror structure is observed by multiple spacecraft. It is difficult to precisely calculate the spatial scale of these mirror structures with observations from a single spacecraft. However, we can still estimate the upper limit of the widths of these structures by assuming that the spacecraft is passing through the center of the structures. This assumption is reasonable for events during which the minimum magnetic field magnitude is very close to zero, for example, the structures between 0810 and 0820 UT on 15 March 2009 (see Figure 3). A second assumption must be made; that is, these structures are stationary in the moving frame of background plasma. Under these two assumptions, we can estimate the width of mirror structures by integrating the background plasma flow. It is noted in both Figures 3 and 5 that the background plasma flow is very small in the *z* direction, which is the major direction of

the magnetic field after the dipolarization. We integrate the x and y components of the plasma flow through the structures. The width of mirror structures is estimated by:

$$Dm = \sqrt{\left(\int_{t1}^{t2} V_x\, dt\right)^2 + \int_{t1}^{t2} V_y\, dt\Big)^2} \quad (2)$$

where Dm is the diameter or width of mirror structures, V_x, and V_y are respectively the x and y components of observed plasma flows, while $t1$ and $t2$ are the times when the magnetic field starts to decline from and return to the background field, respectively. Using this simple integration, we estimate the widths of three deep magnetic holes at 0812, 0814, and 0818 UT, marked by the thick vertical dashed lines in Figure 3. Since the boundaries of these three events are relatively distinct and the minimum field strengths inside these holes are very small, they are suitable for our calculation. The widths (diameters) of three selected mirror structures are 221, 689, and 784 km, respectively. During this interval, the background magnetic field strength is about 8 nT. The gyroradius for a 10 keV proton and electron (both with a 90° pitch angle) are 1818 and 42 km, respectively. Thus the estimated width of the deep magnetic hole is smaller than a proton gyroradius but is several to tens of electron gyroradii. We also need to consider the correction brought by the azimuthal drift of particles on the observed convection velocity of the background plasma. For example, in the dipole field the azimuthal drift velocity of a 10 keV proton with a 90° pitch angle is about 14 km/s and westward. If we subtract this drift velocity from the measured plasma velocity, the width of the three mirror structures are estimated as 428, 102, and 610 km, respectively, which is still substantially smaller than a proton gyroradius. We also find that the widths of the small-amplitude structures right after the dipolariztion are similar, 300–600 km. This result is different from the spatial scale of the mirror structures estimated in other regimes. For example, the width of mirror structures in the solar wind is typically tens of proton gyroradii [*Zhang et al.*, 2008].

[15] The electron distribution during these mirror structures is also interesting. The electron anisotropy is different from that of ions after magnetic field dipolarizations (see Figures 3c and 3d as well as Figures 4c and 4d). Instead of having perpendicular anisotropy as the ions do, the parallel temperature of electrons is generally greater in the background plasma after dipolarizations. We find that this parallel anistropy, however, does not make the plasma unstable to the firehose instability which is often found in parallel-anisotropic plasmas. In Figures 3e and 5e, we can find that the firehose instability threshold is not reached except for two short intervals in Figure 3e. During these two intervals, the anisotropy of electrons is very small and so is the magnetic field strength, which can cause a very large plasma beta value. Thus, these two excursions may be caused by the uncertainty of the difference between two large plasma beta values ($\beta_{\parallel,e}$ and $\beta_{\perp,e}$) and do not suggest firehose instability. The parallel-anisotropic distribution of electrons can be produced by Fermi acceleration when the configuration of magnetic field is significantly changed, especially when the magnetic field lines shorten during dipolarization [*Smets et al.*, 1999; *Sergeev et al.*, 2001; *Wu et al.*, 2006]. Many authors have studied this type of electron parallel anisotropy with plasma measurements from different missions. *Smets et al.* [1999] specifically studied the pitch angle distributions of electrons following the dipolarization of a substorm using Interball-Tail observations. They found that 10 keV electrons have beam-like (along the magnetic field direction), conic-like (with an intermediate pitch angels of about 30°), and perpendicularly peaked distributions at $L \sim 11$, $L \sim 9$, and $L \sim 7$, respectively. They modeled adiabatic acceleration of electrons in the simple model of magnetic field dipolarization and found that, in the region where the magnetic field lines were largely shorter after dipolarizations, Fermi acceleration was the leading process to heat electrons in the parallel direction [*Smets et al.*, 1999; Figure 7], while the betatron heating on electrons, which usually enhanced the perpendicular temperature, only dominated inside of $L \sim 9$. The dominant Fermi acceleration on electrons was also found in AMPTE Ion Release Module (IRM) observations between 10 and 15 R_E in the magnetotail [*Sergeev et al.*, 2001]. *Wu et al.* [2006] used Cluster observations to show the evolution of magnetotail energetic electron pitch angle distributions during substorms. They proposed a model in which Fermi acceleration dominated for electrons that were accelerated from the reconnection region, while betatron acceleration dominated for electrons accelerated from the near-tail region (inside of 10 R_E in tail). These results are consistent with our observations of electron pitch angle distribution after the dipolarizations, suggesting that the THEMIS-observed parallel anisotropy of electrons is mainly caused by Fermi acceleration at ~11 R_E when the length of magnetic field lines suddenly shorten after dipolarizations. The effect of Fermi acceleration is probably more significant for electrons than for ions in this region since the timescale of magnetic field reconfiguration is shorter than the bounce period of ions but longer than or comparable to the bounce period of electrons. Thus, following the strong compression of magnetic field at dipolarization, the betatron heating could dominate the acceleration of ions, producing THEMIS-observed perpendicular anisotropy of ions.

[16] However, within the mirror structures, the electron distribution becomes isotropic despite the anisotropy of the surrounding electrons in the parallel direction to the ambient magnetic field. The clear correlation of isotropic electrons and the mirror structures appears in both events in this study. We propose that these isotropic electrons may come from the pitch angle scattering of wave-particle interaction on the background electrons that are initially anisotropic in the parallel direction, or come from electrons that have different initial pitch angle distributions than the background electrons, or originate in different regimes. In the first event (see Figure 3d), a couple of very short intervals of electron perpendicular anisotropy are observed inside the small-amplitude magnetic holes (0751 UT), providing some clues for the following isotropic electrons. It suggests that these isotropic electrons may come from electrons that are previously heated preferentially in the perpendicular direction. This perpendicular anisotropy can be consumed during the development of the mirror instability or other anisotropy instability [*Gary and Karimabadi*, 2006]. In magnetized plasmas, the electron perpendicular anisotropy can drive two distinct instabilities; that is, electron mirror and whistler

instabilities. Both electron anisotropy instabilities may operate simultaneously and are able to remove the perpendicular anisotropy of electrons. Theoretical studies on the electron temperature anisotropy instabilities [*Gary and Karimabadi*, 2006] have shown that in a collisionless and homogeneous plasma the electron mirror instability has a smaller growth rate and a larger anisotropy threshold than the whistler mode instability. *Gary and Karimabadi* [2006] also pointed out that this relation of different electron anisotropy instabilities is valid over a large range of plasma environments ($0.10 \leq \beta_{\|e} \leq 1000$). This result tells us that in the homogeneous plasma the growth of electron mirror instability, even with perpendicular electron anisotropy, can still be suppressed by other modes and the whistler instability is more likely to grow. However, after the dipolarization and fast plasma flows, the near-tail is strongly disturbed. The plasma in this region may not be a homogeneous plasma and the theoretical analysis of electron anisotropy instability on a homogeneous plasma may not apply. Which instability is responsible for isotropizing the electrons after the dipolarization requires further study.

[17] Nevertheless, these observations suggest a possible connection of electron kinetics with mirror instability in the near-Earth tail, which is hardly reported in the previous studies on the mirror-mode structures in other regions. In the solar wind and the magnetosheath, ions play the dominant role for mirror instability and the width of mirror structures is typically larger than ion gyroradius [*Tsurutani et al.*, 1982; *Zhang et al.*, 2008]. In this study, the electron-gyroradius scale of THEMIS-observed mirror structures and their correlation with the changes of electron pitch angle distribution implies that the effects of electron kinetics on the mirror instability may be significant in the near-Earth plasma sheet. Unfortunately, it is difficult to further examine the electron instability in the current study. Most mirror structures in the two studied events have fully saturated and the perpendicular anisotropy of electrons is only found in very short intervals of developing magnetic holes. Moreover, high-resolution wave measurements are not available during these events for us to examine the whistler waves. The relation of electron dynamics with mirror instability can be further understood with more observations of developing mirror structures and high-resolution wave observations.

5. Discussion

[18] Although mirror structures or mirror waves have been extensively studied in the planetary magnetosheath [e.g., *Tsurutani et al.*, 1982; *Joy et al.*, 2006] and in the solar wind [e.g., *Winterhalter et al.*, 1994; *Zhang et al.*, 2008], there are few investigations of mirror structures inside the Earth's magnetosphere. In this study, we investigate mirror-mode structures at the midnight sector of near-Earth tail after dipolarizations during substorms, which are detected by THEMIS spacecraft. The near-Earth plasma sheet mirror structures have very similar features with those in other regimes. The magnetic field signatures are similar to the magnetic-hole type of mirror structures in the magnetosheath and the solar wind, that is, sporadically distributed magnetic holes appear within a steady and uniform background magnetic field. Inside the mirror structures, the magnetic field is strongly depressed to as low as 3% of the background field strength. The anticorrelation between magnetic field changes and the variations of plasma density shows the mirror-mode nature of these structures. The mirror instability threshold is marginally reached inside these magnetic holes, while the background plasma remains mirror stable. Reaching the marginal mirror instability threshold inside these mirror structures is caused by the large decrease of the magnetic field strength, which greatly enhances the effective plasma beta value in these structures. In the first event studied in this paper, relatively smaller-amplitude magnetic holes are observed immediately after the dipolarization in the anisotropic plasma, although the mirror instability threshold is never reached during these holes.

[19] In this paper, we also investigate the source of mirror-mode structures in the central plasma sheet, which appears to be quite different from sources that produce mirror structures in the magnetosheath and in the solar wind. In magnetized plasmas, the mirror instability is driven by the plasma perpendicular anisotropy [*Hasegawa*, 1969]. Although the ion cyclotron instability can also be driven inside this anisotropic plasma and may be operating at the same time, the compressional signatures of these observed structures show that they are produced by mirror instability because the fluctuations of ion cyclotron instability are predominantly transverse. First we note that the ions in the central plasma sheet are anisotropic immediately after the dipolarizations of the near-Earth tail. The ion anisotropy can provide the free energy for the mirror instability to grow. In fact, after the dipolarization, small-amplitude magnetic holes appear inside the anisotropic ion plasma, which appear to be manifestations of growing mirror structures. These results indicate that the anisotropic ions that appear to be produced by the dipolarization process drive the mirror instability in the near-Earth plasma sheet. Although it is still not fully understood how substorm-associated dipolarization causes the anisotropic ions, our observations appear to be consistent with the previous studies on the plasma anisotropy in the central plasma sheet. It has been reported by *De Michelis et al.* [1999] that the plasma anisotropy in the near-Earth tail region is more often found during geomagnetic active periods. Other observations and analyses on the plasma anisotropy also suggest that the perpendicular ion anisotropy after dipolarizations in substorms were mainly caused by betatron heating when the magnetic field strength is strongly enhanced [*Smets et al.*, 1999; *Wu et al.*, 2006]. This mechanism is similar to the mechanism that produces anisotropy for energetic ions in the inner magnetosphere where the betatron acceleration plays an important role to increase ion perpendicular temperature [*Liu and Rostoker*, 1995; *Woch et al.*, 1988]. In the two events studied in this paper, we show a direct connection between the dipolarization processes, ion anisotropy, and the following mirror structures. The compression of magnetic field accompanied with the dipolarizations is obvious at each dipolarization event, which can heat the ions preferentially in the direction perpendicular to the magnetic field and produce the perpendicular anisotropy of ions. This adiabatic acceleration of ions in the plasma sheet is different from the mechanism for the magnetosheath plasma anisotropy, which comes from the heating of the bow shock [e.g., *Liu et al.*, 2005].

[20] Another important observation in this study is the possible connection of electron dynamics with the near-Earth plasma sheet mirror instability; hardly reported in previous observations of mirror instability. First, we find that the estimated width of mirror structures in the near-Earth tail is smaller than a proton gyroradius or tens of electron gyroradii. Although our method to estimate the mirror structure width is simplified and more precise calculations can be done with multipoint observations using the new THEMIS spacecraft configuration, this finding is still quite surprising since most observed mirror structures in previous studies have a typical width of tens of (at least several) ion gyroradii [e.g., *Zhang et al.*, 2008]. The observation of an electron-gyroradius scale of mirror structures suggests a possible role of electron kinetics in the saturation of mirror instability in the near-Earth plasma sheet.

[21] Moreover, we find that the change of electron pitch angle distribution is strongly correlated with the large-amplitude magnetic holes; that is, electrons become isotropic inside these mirror structures. We notice that after the dipolarization the background electrons have opposite anisotropy to that of ions; the parallel temperature of electrons is larger than the perpendicular temperature. This type of electron pitch angle distribution has also been studied by other authors using different observations, in which Fermi acceleration is found to be a major contributor to the parallel heating of electrons [*Smets et al.*, 1999; *Sergeev et al.*, 2001]. Although the strong enhancement of the magnetic field also provides betatron heating to increase the perpendicular temperature of electrons, Fermi acceleration still dominates the acceleration on electrons at and beyond 10 R_E in tail [*Smets et al.*, 1999; *Sergeev et al.*, 2001]. However, we find that the parallel anisotropy in electrons does not reach the threshold for parallel anisotropy instabilities, such as the firehose instability. Despite this anisotropic background electron plasma, isotropic electrons are found inside of the mirror structures. It is difficult in this study to thoroughly examine how these isotropic electrons form since in the two events studied here we mostly observed the saturated mirror structures and cannot track the evolution of electron distributions. We propose two possible mechanisms to produce the isotropic electrons out of the parallel anisotropic background electron plasma. One explanation is that these isotropic electrons come from the pitch angle scattering of the initially parallel anisotropic electrons inside these mirror structures. Another possible explanation is that these electrons are previously anisotropic in the perpendicular direction and the perpendicular anisotropy is consumed by the growth of mirror instability or another electron instability mode such as whistler mode instability [e.g., *Gary and Karimabadi*, 2006]. We find some suggestive evidence to show that the latter case is more likely in accord with current observations. A short interval of perpendicularly anisotropic electrons are found inside of a couple of small-amplitude magnetic holes before the saturated mirror structures, suggesting that inside the mirror structures the electrons behavior differently from the background electron plasma. The electrons can be initially anisotropic in the perpendicular direction and excite the electron mirror or whistler instability which can consume the perpendicular anisotropy. Thus the mirror structure can also extract free energy from the anisotropic electrons, although the anisotropic ions may dominate the initial growth of mirror instability. These observations imply that in the near-Earth tail electron kinetics may also play a role to affect the growth of mirror instability. The finding that the typical width of magnetic holes is less than an ion gyroradius may suggest that the electrons may also play a role during the saturation of mirror structures. This result indicates that the development of mirror instability in the near-Earth plasma sheet is different from that in previous studies on mirror instability, in which the electrons were considered to have little effect on mirror instability [*Gary and Karimabadi*, 2006; *Pokhotelov et al.*, 2000] and mirror structures usually saturated with a typical scale of tens of ion gyroradius [*Zhang et al.*, 2008]. In the near-Earth tail plasma sheet, both ions and electrons may play roles for the mirror instability, but their effects may dominate in different stages of mirror structures.

[22] Unfortunately, for the two events studied in this paper, high-resolution wave measurements are not available in the mirror structures. Based on the current observations, we cannot examine if whistler waves are excited by the electron anisotropy. We also need more observations of growing/nonsaturated mirror structures to track the evolution of electron pitch angle distributions in order to examine our proposed mechanism for isotropic electrons inside mirror structures and better understand the role of electrons during the growth and saturation of the mirror instability in the near-Earth tail. Nevertheless, since most previous studies on mirror structures only focused on ion kinetics, the current case studies of mirror-mode structures in the near-Earth plasma sheet provide some new observational aspects for mirror-mode instability by showing their possible connection with electron kinetics.

[23] It is also important to note that the magnetic mirror structures reported in this study are embedded in mirror stable plasma; that is, the background plasma remains mirror stable despite the ion anisotropy. A similar phenomenon has also been found in the dayside magnetosheath by THEMIS [*Balikhin et al.*, 2009]; a phenomenon often referred to as "bi-stability" [*Passot et al.*, 2006], that is, magnetic hole-type mirror structures are surrounded by a mirror-stable plasma. Due to the extensive observations in the magnetosheath, the magnetic hole-type mirror structures can be tracked back to the initial growth of mirror instability near the bow shock, where the plasma is strongly mirror unstable and both magnetic peaks and holes develop. The hole-type structures survive as the magnetosheath plasma becomes more mirror stable toward the magnetopause, while the peak-type mirror structures are heavily damped. However, from this study we do not find a region where the plasma is substantially unstable to the mirror instability nor to peak-type mirror structures or quasi-oscillary fluctuations. In the first event, the large-amplitude tail mirror structures are preceded by some relatively smaller-amplitude magnetic holes, which appear in conjunction with the strong magnetic field fluctuations during the dipolarization. These fluctuations may also play an important role for the growth of the mirror structures besides the ion anisotropy; that is, the mirror instability is probably driven by both ion anisotropy

and the highly fluctuating magnetic field from the dipolarization process.

[24] **Acknowledgments.** This research was supported by NASA grant NAS5-02099. We acknowledge C. T. Russell and the THEMIS GBO and EPO teams, I. R. Man and the CARISMA team, the GIMA team, and the CANMOS team for providing the ground magnetic field data. Financial support of DC at the Technical University of Braunschweig by the German Ministerium fur Wirtschaft und Technologie and the Deutsches Zentrum fur Luft- und Raumfahrt under grant 50QP0402 is acknowledged.
[25] Masaki Fujimoto thanks Dan Winske and I. Rae for their assistance in evaluating this manuscript.

References

Angelopoulos, V. (2008), The THEMIS mission, *Space Sci. Rev.*, *141*, 5–34, doi:10.1007/s11214-008-9336-1.

Auster, H. U., et al. (2008), The THEMIS fluxgate magnetometer, *Space Sci. Rev.*, *141*, 235–264, doi:10.1007/s11214-008-9365-9.

Balikhin, M. A., R. Z. Sagdeev, S. N. Walker, O. A. Pokhotelov, D. G. Sibeck, N. Beloff, and G. Dudnikova (2009), THEMIS observations of mirror structures: Magnetic holes and instability threshold, *Geophys. Res. Lett.*, *36*, L03105, doi:10.1029/2008GL036923.

Constantinescu, O. D., K. -H. Glassmeier, R. Treumann, and K. -H. Fornaçon (2003), Magnetic mirror structures observed by Cluster in the magnetosheath, *Geophys. Res. Lett.*, *30*(15), 1802, doi:10.1029/2003GL017313.

Constantinescu, O. D., et al. (2009), THEMIS observations of duskside compressional Pc5 waves, *J. Geophys. Res.*, *114*, A00C25, doi:10.1029/2008JA013519.

Crooker, N. U., and G. L. Siscoe (1977), A mechanism for pressure anisotropy and mirror instability in the dayside mangetosheath, *J. Geophys. Res.*, *82*, 185–186.

De Michelis, P., I. A. Daglis, and G. Consolini (1999), An average image of proton plasma pressure and of current systems in the equatorial plane derived from AMPTE/CCE-CHEM measurements, *J. Geophys. Res.*, *104*, 28,615–28,624.

Gary, S. P., and H. Karimabadi (2006), Linear theory of electron temperature anisotropy instabilities: Whistler, mirror, and Weibel, *J. Geophys. Res.*, *111*, A11224, doi:10.1029/2006JA011764.

Genot, V., E. Budnik, P. Hellinger, T. Passot, G. Belmont, P. M. Travnicek, P. L. Sulem, E. Lucek, and L. Dandouras (2009), Mirror structures above and below the linear instability threshold: Cluster observations, fluid model, and hybrid simulations, *Ann. Geophys.*, *27*, 601–615.

Glassmeier, K., U. Motschmann, C. Mazelle, F. Neubauer, K. Sauer, S. Fuselier, and M. Acua (1993), Mirror modes and fast magnetoacoustic waves near the magnetic pileup boundary of comet P/Halley, *J. Geophys. Res.*, *98*, 20,955–20,964, doi:10.1029/93JA02582.

Haerendel, G. (2000), Outstanding issues in understanding the dynamics of the inner plasma sheet and ring current during storms and substorms, *Inn. Magnetos. Dyn.*, *25*, 2379–2388.

Haerendel, G., W. Baumjohann, E. Georgescu, R. Nakamura, L. M. Kistler, B. Klecker, H. Kucharek, A. Vaivads, T. Mukai, and S. Kokubun (1999), High-beta plasma blobs in the morningside plasma sheet, *Ann. Geophys.*, *17*, 1592–1601.

Haerendel, G., E. Georgescu, K. H. Glassmeier, B. Klecker, Y. V. Bogdanova, H. Rème, and H. Frey (2004), Cluster observes formation of high-beta plasma blobs, *Ann. Geophys.*, *22*, 2391–2401.

Hasegawa, A. (1969), Drift mirror instability in the magnetosphere, *Phys. Fluids*, *12*, 2642–2650.

Hellinger, P., P. Travnicek, A. Mangeney, and R. Grappin (2003), Hybrid simulations of the magnetosheath compression: Marginal stability path, *Geophys. Res. Lett.*, *30*(18), 1959, doi:10.1029/2003GL017855.

Joy, S. P., M. G. Kivelson, R. J. Walker, K. K. Khurana, C. T. Russell, and W. R. Paterson (2006), Mirror-mode structures in the Jovian magnetosheath, *J. Geophys. Res.*, *111*, A12212, doi:10.1029/2006JA011985.

Kivelson, M. G., and D. J. Southwood (1996), Mirror instability: 2. The mechanism of nonlinear saturation, *J. Geophys. Res.*, *101*, 17,365–17,371, doi:10.1029/96JA01407.

Liu, W., and G. Rostoker (1995), Energetic ring current particles generated by recurring substorm cycles, *J. Geophys. Res.*, *100*, 21,897–21,910.

Liu, Y. C. M., M. A. Lee, and H. Kucharek (2005), A quasilinear theory of ion "thermalization" and wave excitation downstream of Earth's bow shock, *J. Geophys. Res.*, *110*, A09101, doi:10.1029/2005JA011096.

Lucek, E. A., M. W. Dunlop, T. S. Horbury, A. Balogh, P. Brown, P. Cargill, C. Carr, K. H. Fornaçon, E. Georgescu, and T. Oddy (2001), Cluster magnetic field observations in magnetosheath: Four-point measurement of mirror structures, *Ann. Geophys.*, *19*, 1421–1428.

Lui, A. T. Y., and D. C. Hamilton (1992), Radial profiles of quiet time magnetospheric parameters, *J. Geophys. Res.*, *97*, 19,325–19,332.

Mann, I. R., et al. (2008), The upgraded CARISMA magnetometer array in the THEMIS era, *Space Sci. Rev.*, *141*, 413–451, doi:10.1007/s11214-008-9457-6.

McFadden, J. P., C. W. Carlson, D. Larson, M. Ludlam, R. Abiad, B. Elliott, P. Turin, M. Marckwordt, and V. Angelopoulos (2008), The THEMIS ESA plasma instrument and in-flight calibration, *Space Sci. Rev.*, *141*, 277–302, doi:10.1007/s11214-008-9440-2.

Mende, S. B., S. E. Harris, H. U. Frey, V. Angelopoulos, C. T. Russell, E. Donovan, B. Jackel, M. Greffen, and L. M. Peticolas (2008), The THEMIS array of ground-based observatories for the study of auroral substorms, *Space Sci. Rev.*, *141*, 357–387, doi:10.1007/s11214-11008-19380-x.

Pantellini, F. G. E., and S. J. Schwartz (1995), Electron-temperature effects in the linear proton mirror instability, *J. Geophys. Res.*, *100*, 3539–3549.

Passot, T., V. Ruban, and P. L. Sulem (2006), Fluid description of trains of stationary mirror structures in a magnetized plasma, *Phys. Plasma*, *13*, 102310, doi:10.1063/1.2356485.

Peticolas, L. M., et al. (2008), The time history of events and macroscale interactions during substorms (THEMIS) education and outreach (E/PO) program, *Space Sci. Rev.*, *141*, 557–583, doi:10.1007/S11214-008-9458-5.

Pokhotelov, O. A., M. A. Balikhin, H. S. Alleyne, and O. G. Onishchenko (2000), Mirror instability with finite electron temperature effects, *J. Geophys. Res.*, *105*, 2393–2401.

Pokhotelov, O. A., O. G. Onishchenko, M. A. Balikhin, R. A. Treumann, and V. P. Pavlenko (2001), Drift mirror instability in space plasmas: 2. Nonzero electron temperature effects, *J. Geophys. Res.*, *106*, 13,237–13,246, doi:10.1029/2000JA000310.

Rae, I. J., I. R. Mann, C. E. J. Watt, and L. M. Kistler (2007), Equator-S observations of drift mirror-mode waves in the dawnside magnetosphere, *J. Geophys. Res.*, *112*, A11203, doi:10.1029/2006JA012064.

Russell, C. T., W. Riedler, K. Schwingenschuh, and Y. Yeroshenko (1987), Mirror instability in the magnetosphere of Comet Halley, *Geophys. Res. Lett.*, *14*, 644–647.

Russell, C. T., M. G. Kivelson, K. K. Khurana, and D. E. Huddleston (1999), Magnetic fluctuations close to Io: Ion cyclotron and mirror-mode wave properties, *Planet. Space Sci.*, *47*, 143–150.

Russell, C. T., P. J. Chi, D. J. Dearborn, Y. S. Ge, B. Kuo-Tiong, J. D. Means, D. R. Pierce, K. M. Rowe, and R. C. Snare (2008), THEMIS ground-based magnetometers, *Space Sci. Rev.*, *141*, 384–412, doi:10.1007/s11214-008-9337-01.

Russell, C. T., X. Blanco-Cano, L. K. Jian, and J. G. Luhmann (2009), Mirror-mode storms: STEREO observations of protracted generation of small amplitude waves, *Geophys. Res. Lett.*, *36*, L05106, doi:10.1029/2008GL037113.

Sergeev, V. A., W. Baumjohann, and K. Shiokawa (2001), Bi-directional electron distributions associated with neartail flux transport, *Geophys. Res. Lett.*, *28*, 3813–3816.

Smets, R., D. Delcourt, J. Sauvaud, and P. Koperski (1999), Electron pitch angle distributions following the dipolarization phase of a substorm: Interball-Tail observations and modeling, *J. Geophys. Res.*, *104*, 14,571–14,581, doi:10.1029/1998JA900162.

Southwood, D. J., and M. G. Kivelson (1993), Mirror instability: 1. The physical mechanism of linear instability, *J. Geophys. Res.*, *98*, 9181–9187.

Soucek, J., E. Lucek, and I. Dandouras (2008), Properties of magnetosheath mirror modes observed by Cluster and their response to changes in plasma parameters, *J. Geophys. Res.*, *113*, A04203, doi:10.1029/2007JA012649.

Stevens, M. L., and J. C. Kasper (2007), A scale-free analysis of magnetic holes at 1 AU, *J. Geophys. Res.*, *112*, A05109, doi:10.1029/2006JA012116.

Tajiri, M. (1967), Propagation of hydromagnetic waves in collisionless plasma, part II: Kinetic approach, *J. Phys. Soc. Jpn.*, *22*, 1482–1494.

Travnicek, P., P. Hellinger, M. G. G. T. Taylor, C. P. Escoubet, I. Dandouras, and E. Lucek (2007), Magnetosheath plasma expansion: Hybrid simulations, *Geophys. Res. Lett.*, *34*, L15104, doi:10.1029/2007GL029728.

Tsurutani, B. T., E. J. Smith, R. R. Anderson, K. W. Ogilvie, J. D. Scudder, D. N. Baker, and S. J. Bame (1982), Lion roars and nonoscillatory drift mirror waves in the magnetosheath, *J. Geophys. Res.*, *87*, 6060–6072.

Tsurutani, B. T., G. S. Lakhina, E. J. Smith, B. Buti, S. L. Moses, F. V. Coroniti, A. L. Brinca, J. A. Slavin, and R. D. Zwickl (1999), Mirror-mode structures and ELF plasma waves in the Giacobini-Zinner magnetosheath, *Nonlinear Processes Geophys.*, *6*, 229–234.

Vaivads, A., W. Baumjohann, G. Haerendel, R. Nakamura, H. Kucharek, B. Klecker, M. R. Lessard, L. M. Kistler, T. Mukai, and A. Nishida (2001), Compressional Pc5 type pulsations in the morningside plasma sheet, *Ann. Geophys.*, *19*, 311–320.

Volwerk, M., T. L. Zhang, M. Delva, Z. Vörös, W. Baumjohann, and K. -H. Glassmeier (2008), Mirror-mode-like structures in Venus' induced magnetosphere, *J. Geophys. Res.*, *113*, E00B16, doi:10.1029/2008JE003154.

Winterhalter, D., M. Neugebauer, B. E. Goldstein, E. J. Smith, S. J. Bame, and A. Balogh (1994), Ulysses field and plasma observations of magnetic holes in the solar wind and their relation to mirror-mode structures, *J. Geophys. Res.*, *99*, 23,371–23,381.

Woch, J., G. Kremser, A. Korth, O. A. Pokhotelov, V. A. Pilipenko, Y. M. Nezlina, and E. Amata (1988), Curvature-driven drift mirror instability in the magnetosphere, *Planet. Space Sci.*, *36*, 383–393.

Wu, P., T. A. Fritz, B. Larvaud, and E. Lucek (2006), Substorm associated magnetotail energetic electrons pitch angle evolutions and flow reversals: Cluster observation, *Geophys. Res. Lett.*, *33*, L17101, doi:10.1029/2006GL026595.

Zhang, T. L., et al. (2008), Characteristic size and shape of the mirror-mode structures in the solar wind at 0.72 AU, *Geophys. Res. Lett.*, *35*, L10106, doi:10.1029/2008GL033793.

Zhang, T. L., W. Baumjohann, C. T. Russell, L. K. Jian, C. Wang, J. B. Cao, M. Balikhin, X. Blanco-Cano, M. Delva, and M. Volwerk (2009), Mirror-mode structures in the solar wind at 0.72 AU, *J. Geophys. Res.*, *114*, A10107, doi:10.1029/2009JA014103.

Zhu, X. M., and M. G. Kivelson (1991), Compressional Ulf waves in the outer magnetosphere: 1. Statistical study, *J. Geophys. Res.*, *96*, 19,451–19,467.

Zhu, X. M., and M. G. Kivelson (1994), Compressional Ulf waves in the outer magnetosphere: 2. A case study of Pc-5 type wave activity, *J. Geophys. Res.*, *99*, 241–252.

V. Angelopoulos, Institute of Geophysics and Planetary Physics, University of California, Los Angeles, 603 Charles E. Young Dr., E, Los Angeles, CA 90065-1567, USA.

O. D. Constantinescu, Institut für Geophysik und Meteorologie, Technische Universität Braunschweig, Braunschweig, D-38092, Germany.

Y. S. Ge and J. Raeder, Space Science Center, 245G Morse Hall, 8 College Rd., University of New Hampshire, Durham, NH 03824, USA. (yasong.ge@gmail.com)

D. Larson and M. P. McFadden, Space Science Laboratory, University of California Berkeley, 7 Gauss Way, Berkeley, CA 94720-7450, USA.